

# Petrography and Origin of Metasediments in the Odienné and Touba Area (NW Côte d'Ivoire)

Gnègnègnima Thomas Koné<sup>1\*</sup>, Alain Nicaise Kouamelan<sup>2</sup>, Augustin Yao Koffi<sup>2</sup>, Jean-Luc Herve Fossou Kouadio<sup>2</sup>, Tokpa Kakeu Lionel Dimitri Boya<sup>2</sup>, Pohn Martial Koffi Adingra<sup>2</sup>

<sup>1</sup>Laboratoire des Sciences, Ressources Minérales et Energétiques (LSRME), Ecole Doctorale Sciences, Technologie et Agriculture Durable (ED-STAD), Université Félix Houphouët-Boigny Abidjan-Cocody, Abidjan, Côte d'Ivoire

<sup>2</sup>Laboratoire de Géologie et Ressources Minières (LGRM), UFR des Sciences de la Terre et des Ressources Minières (UFR-STRM), Université Félix Houphouët-Boigny Abidjan-Cocody, Abidjan, Côte d'Ivoire

Email: \*thomaskone89@gmail.com

**How to cite this paper:** Koné, G.T., Kouamelan, A.N., Koffi, A.Y., Kouadio, J.-L.H.F., Boya, T.K.L.D. and Adingra, P.M.K. (2025) Petrography and Origin of Metasediments in the Odienné and Touba Area (NW Côte d'Ivoire). *Open Journal of Geology*, 15, 265-284.

<https://doi.org/10.4236/ojg.2025.155013>

**Received:** April 15, 2025

**Accepted:** May 23, 2025

**Published:** May 26, 2025

Copyright © 2025 by author(s) and Scientific Research Publishing Inc. This work is licensed under the Creative Commons Attribution International License (CC BY 4.0).

<http://creativecommons.org/licenses/by/4.0/>



Open Access

## Abstract

The study area encompasses the Odienné and Touba sectors in northwestern Côte d'Ivoire. It is located in the Archean-Paleoproterozoic Transition Zone (APTZ), the major structure of which, the Sassandra Shear Zone (SSZ) trending NS then NW-SE, moulds the Archean core (or nucleus). The main lithologies occurring in this region include metasediments, gneisses (migmatites and mylonites), metabasites, and granitoids. This paper highlights new data on the petrographic characteristics and geochemical signature of the metasediments from northwestern Côte d'Ivoire. Field observations and petrographic studies reveal that the metasediments consist of mylonitic-textured quartzite, sillimanite paragneiss, and quartz-rich micaschists, along with garnets or amphibole. Geochemical data has enabled us to narrow down the origin of the metasediment rocks: one sample mainly consists of litharenite sandstone. They also show that their protoliths are basaltic, andesitic, granodioritic, and granitic rocks that are moderately to slightly altered ( $50 < AIC < 65$ ) and that they were emplaced in a tectonic environment that could be of the island arc margin and/or continental margin type.

## Keywords

Odienné, Touba, Archean-Proterozoic Transition, Metasediments, Petrography, Geochemistry

## 1. Introduction

The northwest of Côte d'Ivoire has been studied intending to reveal all the petrogeochemical characteristics and the tectono-metamorphic evolution of the litho-

logical units [1]-[3]. The mapped lithological units are orthogneisses, quartzites with magnetites and amphibolites located to the west of Sassandra Shear Zone (SSZ) (Odienné region), which are, considered to be either ante-Eburnian rocks or early rocks in the Eburnian cycle [3]. For this author, the Eburnian volcanism of Odienné is characterised by the presence of a volcanic and volcano-sedimentary complex [3] [4]. However, the Odienné area could be divided into three domains: (i) the western domain comprising metabasalts, metasediments, a volcanic complex (2.1 Ga) and deformed or undeformed plutons; (ii) the middle domain, which primarily consists of high-temperature paragneisses, mylonites, and ultramylonites; and (iii) the eastern domain comprising silico-clastic and volcanoclastic metasediments with anatexis conditions at the limit of the Tiémé batholith [1]. They concluded that these three domains were juxtaposed by horizontal movements, essentially senestial, sliding along the SSZ. Most of these volcano-sedimentary units are intruded by granitoids and dolerite dykes (or metabasites) [1] [3]. Geochemical studies carried out in the northwest show that most of the metasediments in this zone correspond to siliceous metasediments, metapelites, and paragneisses derived from greywackes [1] [3]. The West African Craton's greenstone belt formations, which are rich in gold mineralization, are made up of a metasedimentary series associated with metavolcanic rocks that have been intruded by granitoids [5]. They are considered to be the hotter and deeper (15 km) portion of the Birimian crust, characterised by high-temperature prograde metamorphism with low-pressure anatexis ( $\approx 5$  Kbars;  $700^\circ < T < 800^\circ$ ) [1]. Furthermore, these metasediments and/or paragneisses of the central subdomain or SSZ are thought to have been emplaced in a vertical accretionary environment above a thinned ancient Archean crust [1] [6]. The present research aims to ascertain the nature, origin, and emplacement context of the metasediments in northwest Côte d'Ivoire using petrographic and geochemical analysis. This detailed study of the metasediments in the northwest at the transition between the Kenema-Man nucleus (Archean) and the Paleoproterozoic belt of the Baoulé-Mossi domain contributes to a better understanding of the petrography, geochemistry, and emplacement conditions of northwest Côte d'Ivoire's metasedimentary units.

## 2. Geological Setting

Côte d'Ivoire belongs to the West African Craton and more specifically to the Léo-Man ridge [7]-[10] (Figure 1). Its geology is mainly characterised by a basement of Precambrian age (Archean and Paleoproterozoic) which covers 97.5% of the territory and a recent sedimentary basin (secondary to Quaternary) covering the remaining 2.5% of this territory [4] (Figure 2).

The Archean domain is made up of ancient formations structured during the Leonian (3.4 - 3.0 Ga) and Liberian (2.9 - 2.7 Ma) orogenies [6] [11]-[16] (Figure 1 and Figure 2). It is characterised by two main groups including a basic complex essentially consisting of grey granulitic gneisses of the TTG type, migmatitic in places (first group), and a second group primarily made up of belts of supracrustal

rocks [12] [17] [18]. Granites and charnockites are associated with these two groups either in the form of intrusions or as anatexitic mobilisates [8] [14] [19] with an overprint of the Eburnian orogeny [20]-[25]. The term “quartzite complex” is used to designate supracrustal rocks composed of kinzigitic metasediments, magnetite quartzites, and granulitic basic rocks [12].

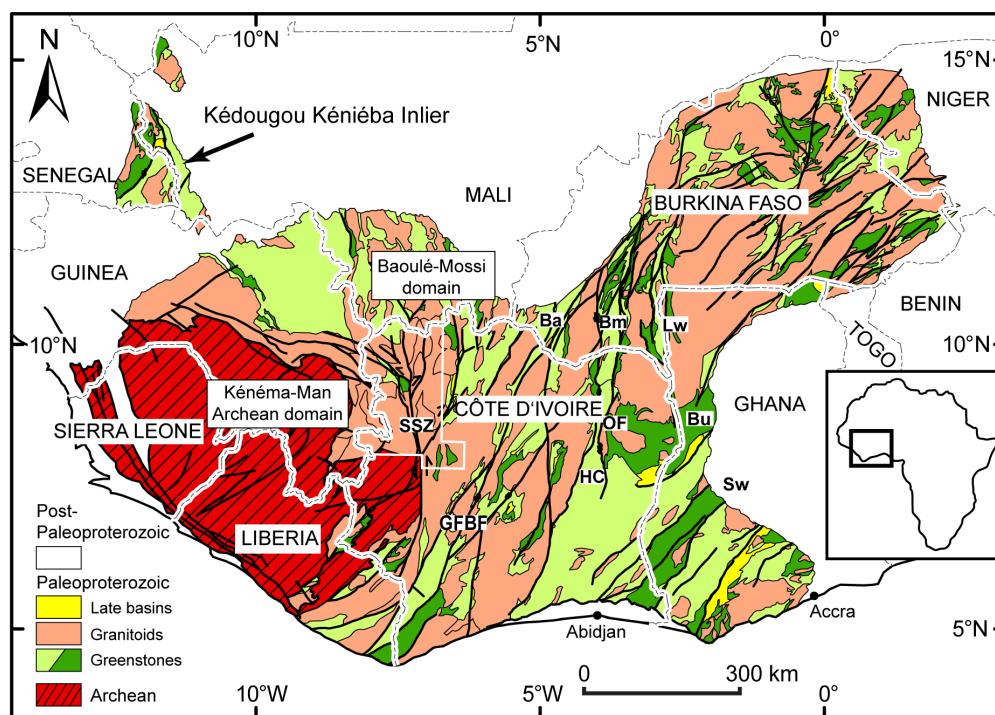


**Figure 1.** Simplified geological map of the Léo-Man Dorsal (modified after [34] [35]). The Paleoproterozoic greenstone belts are divided into light green (volcaniclastic and intermediate to acid volcanic sediments) and dark green (intermediate volcanic lavas and products). **SF** or **SSZ** (Sassandra fault or Shear Zone), **GFBF** (Greenville-Ferkéssédougou-Bobo-Dioulasso Fault), **HC** (Haute Comoé basin), **OF** (Ouango-Fitini belt), **Bu** (Bui belt), **Sw** (Sefwi belt), **Ba** (Banfora belt), **Bm** (Bambéla basin) and **Lw** (Lawa belt) [5].

The Paleoproterozoic domain, also known as the Baoulé-Mossi domain, lies to the east of the SSZ and encompasses the majority of the Ivorian Precambrian basement. Several investigations conducted in this area regarding its structuring have given rise to various controversies. Some work show that this structuring took place during the Eburnian megacycle (2.5 to 1.6 Ga; [9] [26] [27]) with tectonometamorphic phenomena occurring between 2.2 Ga and 2.0 Ga [28]. However, others describe a division into two orogenic cycles, including the Burkinian (2.4 to 2.15 Ga), characterized by tangential tectonics, and the strict Eburnian (2.15 to 1.6 Ga) [29]. The Baoulé Mossi domain records ages between 2.4 and 1.8 Ga with juvenile formations and differentiation of the mantle, according to model ages between 2.5 Ga and 2.2 Ga [30] [31]. The Birimian formations (greenstone belts and granito-gneissic areas) form grooves generally oriented NE-SW and also contain intrusive granitoids [32]. Between the Archean domain and longitude 6°W,

an Archean-Proterozoic transition domain is defined in Ivory Coast, characterized by negative neodymium epsilons, inherited zircons and Archean relics [8]. Finally, thanks to the thermobarometric study in the paragneisses (dated to the Archean), high-grade granulitic metamorphism was highlighted in the Paleoproterozoic domain of the SASSA sector or Sassandra-Cavally river sector (south of our study area) [33].

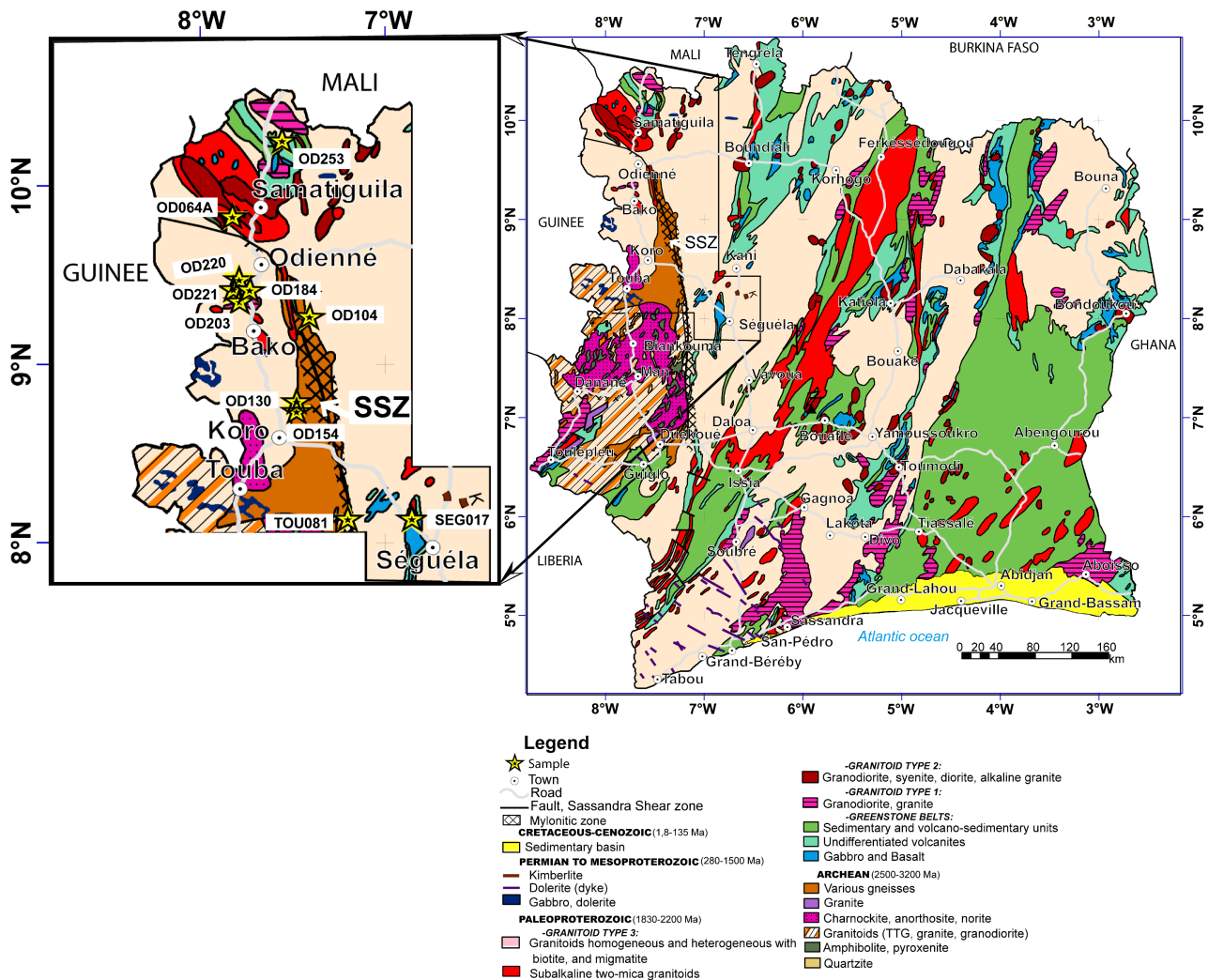


Figure 2. Simplified geological map of Côte d'Ivoire, modified from [9].

### 3. Methodologies

#### 3.1. Sampling

Several fieldworks studies have revealed eleven (11) metasediment outcrops in the Odienné, Touba and Séguéla regions. The process consisted of: (i) observing and describing the outcrops, followed by (ii) sampling a portion as a control and for future analysis. Various samples were observed and collected, including meta-conglomerates, micaschists, migmatitic paragneisses and mylonitised quartzites, the coordinates of which are given in Table 1. These rocks are mainly affected by

E-W and N-S to NW-SE structural deformation of the Sassandra Shear Zone (SSZ). We selected and described seven (7) samples, representative in terms of petrographic facies of the study area and for total rock geochemical analyses, in order to ensure good spatial coverage of the study area. Thin sections of the metasediments were prepared and studied under an Optika B-383POL polarising microscope coupled to a camera at the Geology and Mineral Resources Laboratory of the Université Félix Houphouët Boigny d'Abidjan-Cocody (Côte d'Ivoire). The acronyms used for the abbreviation of minerals are those of [27].

### 3.2. Analytical Method

Geochemical analyses of major and trace elements (Table 1 and Table 2) were carried out at the Bureau Veritas Canada laboratory. Major elements were determined by fluorescence spectrometry and trace elements by LA ICP-MS (Laser Ablation Inductively Coupled Plasma Mass Spectrometry) (Table 1 and Table 2).

Loss on ignition (LOI1000 in %wt) was determined using a robotised TGA system (u351194\_ABJ23001030; <https://www.bureauveritas.ci/>).

**Table 1.** Geographic coordinates and geochemical data (major elements) for metasedimentary rocks in the north-western belt of Côte d'Ivoire.

| Samples  | OD064A   | OD104    | OD130    | SEG017    | OD184     | OD154     | OD220     | OD221     | OD203     | TOU081    | OD253     |
|--|----------|----------|----------|-----------|-----------|-----------|-----------|-----------|-----------|-----------|-----------|
| Lat  | 9.76841  | 9.32155  | 8.79326  | 8.1049966 | 9.31579   | 8.784607  | 9.337943  | 9.338803  | 9.313008  | 8.07891   | 10.19429  |
| Long   | -7.72265 | -7.29574 | -7.38403 | -6.796107 | -7.655202 | -7.381868 | -7.656923 | -7.655191 | -7.648182 | -7.110866 | -7.542159 |
| SiO <sub>2</sub>   | 65.94    | 62.81    | 66.2     |           | 68.7      |           | 66.1      | 75.08     | 53.47     | 68.96     |           |
| Al <sub>2</sub> O <sub>3</sub>   | 17.16    | 14.7     | 15.25    |           | 15.75     |           | 15.85     | 12.24     | 15.58     | 14.09     |           |
| CaO  | 3.76     | 3.83     | 2.12     |           | 0.73      |           | 3.85      | 1.2       | 9.77      | 1.44      |           |
| Fe <sub>2</sub> O <sub>3</sub>   | 3.9      | 7.11     | 5.71     |           | 2.59      |           | 5.25      | 3.85      | 8.77      | 4.45      |           |
| K <sub>2</sub> O   | 1.79     | 3.37     | 2.46     |           | 7.46      |           | 3.03      | 1.91      | 1.35      | 3.01      |           |
| MgO  | 1.47     | 3.1      | 2.48     |           | 1.16      |           | 1.42      | 0.61      | 5.05      | 1.58      |           |
| Na <sub>2</sub> O  | 4.35     | 3.27     | 3.62     |           | 1.35      |           | 3.14      | 4.1       | 3.98      | 4.5       |           |
| P <sub>2</sub> O <sub>5</sub>  | 0.153    | 0.197    | 0.152    |           | 0.152     |           | 0.156     | 0.064     | 0.21      | 0.145     |           |
| SO <sub>3</sub>  | 0.198    | 0.084    | 0.392    |           | 0.027     |           | 0.009     | 0.107     | -0.001    | 1.03      |           |
| TiO <sub>2</sub>   | 0.4      | 0.65     | 0.53     |           | 0.52      |           | 0.6       | 0.27      | 0.86      | 0.38      |           |
| MnO  | 0.04     | 0.12     | 0.07     |           | 0.04      |           | 0.13      | 0.13      | 0.2       | 0.08      |           |
| Cl   | 0.002    | -0.001   | 0.002    |           | 0.008     |           | 0.011     | 0.007     | 0.012     | 0.006     |           |
| LOI1000  | 0.79     | 0.71     | 0.94     |           | 0.93      |           | 0.52      | 0.34      | 0.44      | 1.17      |           |
| Total  | 100.23   | 100.25   | 100.09   |           | 99.72     |           | 100.25    | 100.04    | 99.89     | 101.13    |           |
| CIA  | 63.41    | 58.40    | 65.68    |           | 62.28     |           | 62.93     | 61.27     | 50.78     | 61.15     |           |
| K <sub>2</sub> O + Na <sub>2</sub> O   | 6.14     | 6.64     | 6.08     |           | 8.81      |           | 6.17      | 6.01      | 5.33      | 7.51      |           |
| Log(SiO <sub>2</sub> /Al <sub>2</sub> O <sub>3</sub> )                       | 0.58     | 0.63     | 0.64     |           | 0.64      |           | 0.62      | 0.79      | 0.54      | 0.69      |           |
| Log(Fe <sub>2</sub> O <sub>3</sub> /K <sub>2</sub> O)                        | 0.34     | 0.32     | 0.37     |           | -0.46     |           | 0.24      | 0.30      | 0.81      | 0.17      |           |
| DF 1   | 3.72     | -0.67    | -0.02    |           | -8.22     |           | 1.59      | 0.36      | 4.32      | -0.71     |           |
| DF 2   | 2.48     | 0.45     | -0.04    |           | 5.45      |           | 2.22      | 1.75      | -1.27     | 2.94      |           |
| K <sub>2</sub> O/Na <sub>2</sub> O   | 0.41     | 1.03     | 0.68     |           | 5.53      |           | 0.96      | 0.47      | 0.34      | 0.67      |           |
| Al <sub>2</sub> O <sub>3</sub> /(CaO + Na <sub>2</sub> O + K <sub>2</sub> O) | 1.73     | 1.40     | 1.86     |           | 1.65      |           | 1.58      | 1.70      | 1.03      | 1.57      |           |

**Table 2.** Geochemical data (trace elements) for metasedimentary rocks in the north-western belt of Côte d'Ivoire.

| Samples   | OD064A | OD104 | OD130 | OD184 | OD220 | OD221 | TOU081 |
|-----------|--------|-------|-------|-------|-------|-------|--------|
| <b>Ag</b> | -0.1   | -0.1  | 0.2   | -0.1  | -0.1  | 0.2   | -0.1   |
| <b>As</b> | 0.4    | -0.2  | 506   | 0.4   | 0.6   | 3.0   | 0.4    |
| <b>Ba</b> | 928    | 1100  | 327   | 1640  | 761   | 305   | 1470   |
| <b>Be</b> | 1.6    | 1.6   | 1.2   | 4.2   | 2.0   | 1.2   | 2.0    |
| <b>Bi</b> | 0.04   | 0.08  | 0.76  | 0.06  | 0.02  | 0.1   | 0.14   |
| <b>Cd</b> | 0.2    | 0.1   | -0.1  | -0.1  | 0.2   | 0.7   | -0.1   |
| <b>Ce</b> | 47.2   | 47.8  | 52.0  | 159   | 63.0  | 63.6  | 53.2   |
| <b>Co</b> | 7.8    | 22.4  | 41.3  | 3.3   | 7.1   | 2.5   | 12.5   |
| <b>Cr</b> | 36     | 165   | 139   | 5     | 2     | 5     | 51     |
| <b>Cs</b> | 4.14   | 3.31  | 2.51  | 4.0   | 4.84  | 3.12  | 0.63   |
| <b>Cu</b> | 16     | 52    | 66    | 12    | 16    | 32    | 18     |
| <b>Dy</b> | 1.36   | 3.14  | 2.75  | 4.95  | 7.82  | 7.49  | 2.11   |
| <b>Er</b> | 0.62   | 1.91  | 1.65  | 2.77  | 4.96  | 4.95  | 1.16   |
| <b>Eu</b> | 0.99   | 1.16  | 1.08  | 1.79  | 1.54  | 1.16  | 1.04   |
| <b>Ga</b> | 21.8   | 18.2  | 16.6  | 16.6  | 21.0  | 14.0  | 16.3   |
| <b>Gd</b> | 2.41   | 3.63  | 3.43  | 6.57  | 7.22  | 7.09  | 3.06   |
| <b>Hf</b> | 4.08   | 3.77  | 4.0   | 11.2  | 6.09  | 7.06  | 3.82   |
| <b>Ho</b> | 0.27   | 0.66  | 0.57  | 0.97  | 1.72  | 1.71  | 0.41   |
| <b>In</b> | -0.05  | -0.05 | -0.05 | -0.05 | -0.05 | 0.05  | -0.05  |
| <b>La</b> | 22.6   | 23.8  | 25.7  | 78.8  | 31.7  | 31.6  | 28.5   |
| <b>Lu</b> | 0.08   | 0.26  | 0.23  | 0.41  | 0.7   | 0.74  | 0.16   |
| <b>Mn</b> | 400    | 1050  | 652   | 305   | 968   | 936   | 543    |
| <b>Mo</b> | 0.6    | 0.8   | 2.8   | 2.8   | 0.4   | 1.0   | 1.8    |
| <b>Nb</b> | 7.12   | 8.08  | 6.9   | 31.1  | 13.0  | 14.4  | 7.95   |
| <b>Nd</b> | 21.6   | 22.9  | 23.6  | 61.8  | 33.1  | 31.2  | 23.1   |
| <b>Ni</b> | 16     | 64    | 70    | -2    | -2    | 10    | 14     |
| <b>Pb</b> | 8      | 10    | 5     | 21    | 9     | 68    | 11     |
| <b>Pr</b> | 5.78   | 5.96  | 6.32  | 18.6  | 8.31  | 8.06  | 6.37   |
| <b>Rb</b> | 62.2   | 109   | 94.6  | 265   | 86.4  | 58.4  | 77.5   |
| <b>Re</b> | -0.01  | -0.01 | -0.01 | -0.01 | -0.01 | -0.01 | -0.01  |
| <b>Sb</b> | -0.1   | -0.1  | 1.2   | 0.2   | 1.4   | 1.6   | -0.1   |
| <b>Sc</b> | 5.6    | 16.3  | 13.3  | 6.5   | 14.9  | 10.2  | 8.0    |
| <b>Se</b> | -5     | -5    | -5    | -5    | -5    | -5    | -5     |
| <b>Sm</b> | 3.69   | 4.34  | 4.49  | 10.2  | 7.33  | 7.09  | 4.13   |
| <b>Sn</b> | 0.8    | 1.0   | 1.2   | 2.2   | 2.0   | 1.8   | 1.8    |
| <b>Sr</b> | 897    | 442   | 227   | 266   | 87.2  | 75.9  | 387    |

Continued

|           |      |      |      |      |      |      |      |
|-----------|------|------|------|------|------|------|------|
| <b>Ta</b> | 0.37 | 0.52 | 0.51 | 1.69 | 0.9  | 0.94 | 0.54 |
| <b>Tb</b> | 0.29 | 0.54 | 0.49 | 0.91 | 1.23 | 1.17 | 0.36 |
| <b>Te</b> | -0.2 | -0.2 | -0.2 | -0.2 | -0.2 | -0.2 | -0.2 |
| <b>Th</b> | 4.39 | 4.65 | 5.67 | 24.2 | 7.19 | 8.31 | 5.65 |
| <b>Ti</b> | 2610 | 4190 | 3460 | 3060 | 3560 | 1610 | 2280 |
| <b>Tl</b> | 0.4  | 0.4  | 0.2  | 1.0  | 0.4  | 0.4  | 0.4  |
| <b>Tm</b> | 0.09 | 0.27 | 0.23 | 0.39 | 0.69 | 0.73 | 0.16 |
| <b>U</b>  | 1.98 | 1.27 | 1.62 | 6.92 | 1.64 | 2.25 | 1.47 |
| <b>V</b>  | 49.2 | 156  | 98.5 | 21.5 | 37.1 | 10.2 | 53.8 |
| <b>W</b>  | 0.5  | 1.0  | 3.5  | 3.0  | 3.0  | 1.0  | 0.5  |
| <b>Y</b>  | 6.9  | 17.1 | 15.2 | 26.0 | 47.0 | 43.1 | 10.9 |
| <b>Yb</b> | 0.6  | 1.83 | 1.58 | 2.83 | 4.86 | 5.06 | 1.18 |
| <b>Zn</b> | 85   | 65   | 30   | 40   | 75   | 215  | 35   |
| <b>Zr</b> | 150  | 135  | 146  | 474  | 228  | 257  | 135  |
| <b>Hg</b> |      |      |      |      |      |      |      |
| <b>Li</b> |      |      |      |      |      |      |      |
| <b>Ge</b> |      |      |      |      |      |      |      |

## 4. Results

### 4.1. Petrographic Descriptions

The metasediments selected for this study are micaschists, paragneisses, and mylonitized quartzites located in two distinct metasedimentary units.

#### 4.1.1. Metasedimentary Units West of the SSZ

Most of the metasediments in the western sector are affected by EW-trending, sub-vertical, penetrative schistosity (**Figure 2**). Three micaschists are described in the metasediments located to the west of the SSZ.

- Micaschist OD184 was intruded by granodiorite and metabasite (**Figure 3(a)** and **Figure 3(b)**) during deformation. It has a fine texture and a grayish color, and its mineralogy primarily consists of microcrystals of quartz and plagioclase (around 65%), with bands of micas (muscovite and biotite at around 33%) (**Figure 3(c)**). The mineralogy of this rock is dominated by quartz and micas. (**Figure 3(c)**).
- The garnet micaschists OD220 and OD221 are about two hundred metres apart. OD220 is folded with NW-trending schistosity (**Figure 3(d)**). OD221 is highly silicified, with peritectite garnet in the siliceous zones. Quartz veins cut the schistosity of the garnet micaschists OD220 and OD221 (**Figure 3(f)**). Microscopically, these rocks have a granolepidoblastic texture, with an abundance of small subautomorphic to automorphic quartz and feldspar crystals (around 70%) and elongated greenish-brown biotite crystals, sometimes in clusters highlighting the schistosity (around 25%) (**Figure 3(e)** and **Figure**

**3(g)**). Garnets are visible, and small muscovite crystals and opaque minerals are also present (**Figure 3(g)**).

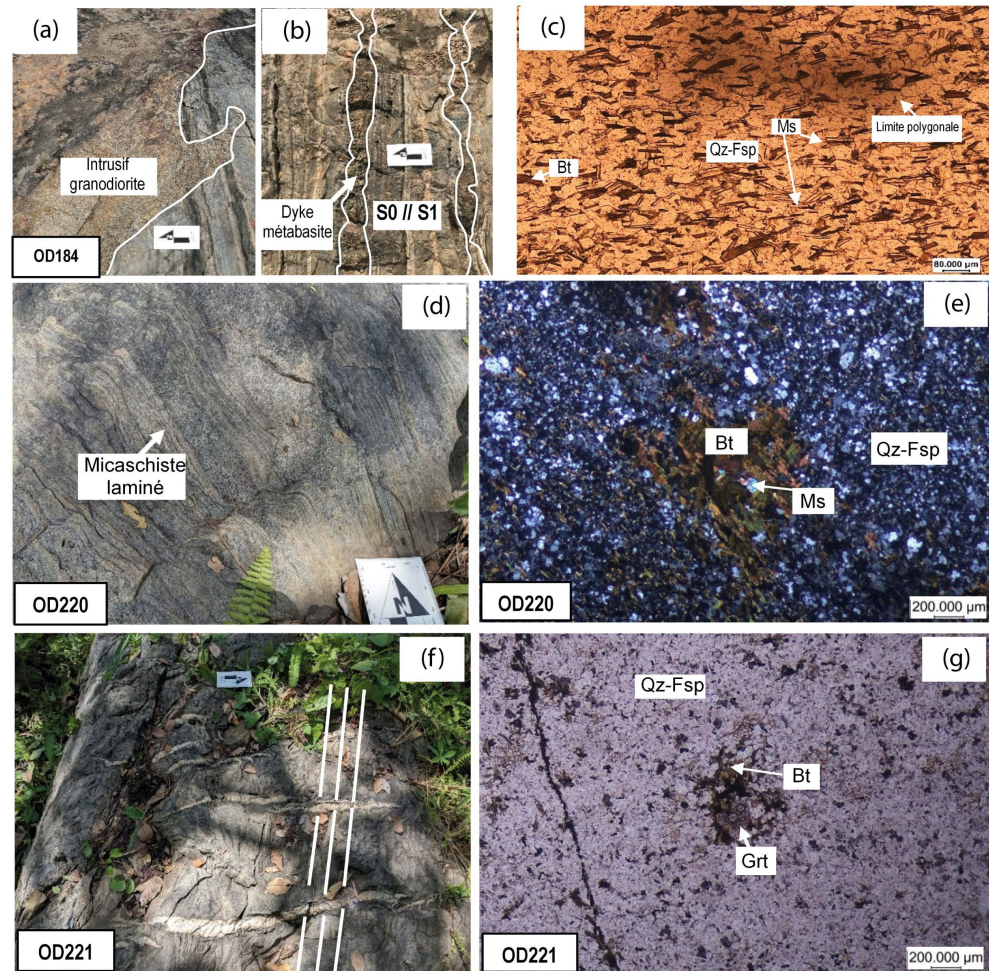


**Figure 3.** Photography and microphotography (under transmitted light) of the metasediments. ((a), (b) and (c)): Outcrop and mineralogy of the mica meta-wacke; ((d) and (e)): Outcrop and mineralogy of the mica meta-wacke; ((f) and (g)): Outcrop and mineralogy of the garnet metawacke-litharenite. Quartz (Qz), Biotite (Bt), Feldspar (Fsp), Plagioclase (Pl), Microcline (Mcc), Chlorite (Chl), Muscovite (Ms), and Garnet (Grt); minerals' abbreviations are according to [27].

#### 4.1.2. Metasedimentary Units within the SSZ

Most of the metasediments in this subdomain are affected by a penetrative schistosity oriented NS to NW-SE (**Figure 2**). Two-mica schists, paragneiss, and mylonite are described in the metasediments located within the SSZ.

- The sillimanite-bearing migmatitic paragneiss OD064A is observed in a quarry 34 km northwest of Odienné. The rock is blackish and exhibits a syn-migmatitic banding oriented NW and characterized by numerous deformed quartz-feldspathic leucosomes (**Figure 4(a)**). Under transmitted light microscopy, this syn-migmatitic banding is highlighted by a preferential orientation of feldspar porphyroclasts (approximately 25%), and biotite rods associated with deformed sillimanite streaks (approximately 42%) (**Figure 4(b)**). Quartz crystals,

approximately 30% of abundance, are generally small and correspond to re-crystallized sub-grains, and are moderately abundant. A few muscovite rods occasionally crosscut the banding, along with tourmaline as an accessory phase in the rock (**Figure 4(b)**).

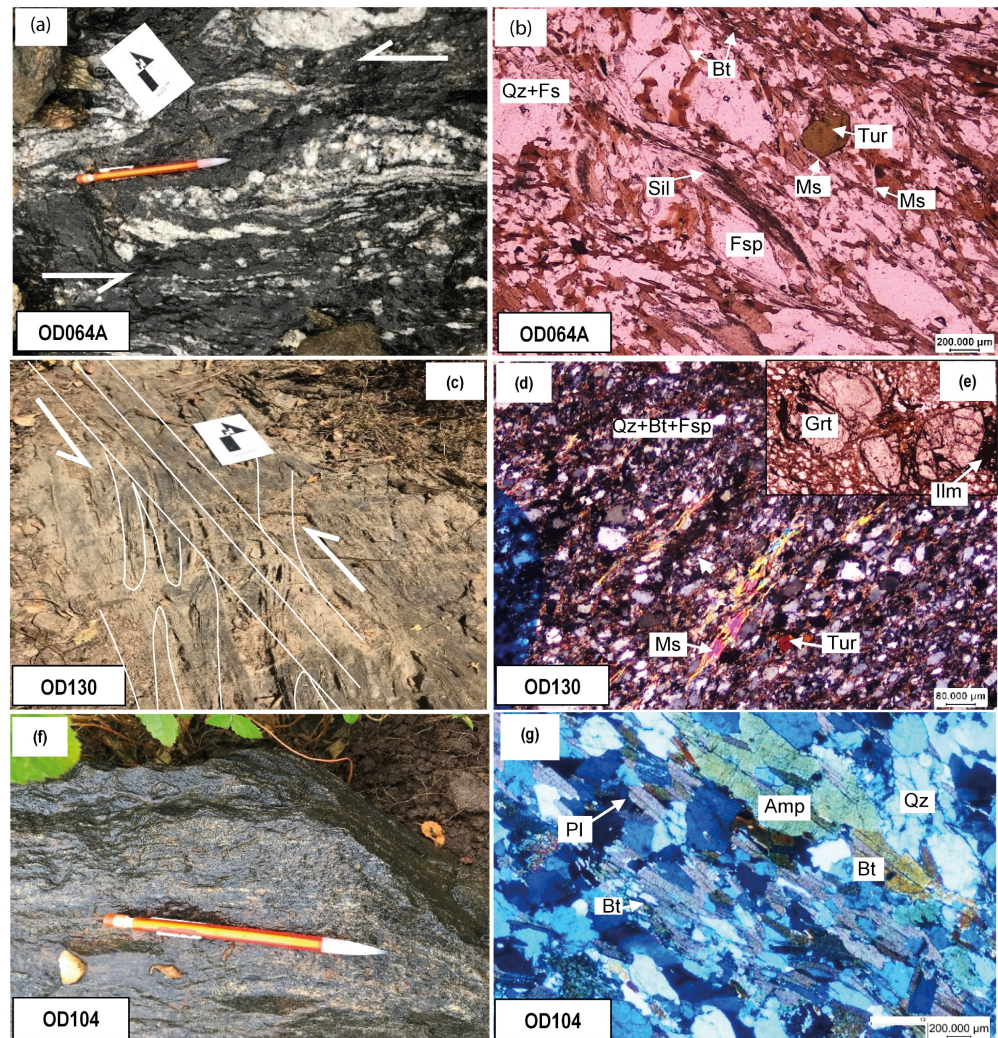


**Figure 4.** Photography and microphotography (under transmitted light) of mica-schists (OD104 and OD130) and migmatitic paragneiss (OD064A): ((a) and (b)): Outcrop and mineralogy of sillimanite paragneiss; ((c) and (d)): Outcrop and mineralogy of micas meta-wacke; ((f) and (g)): Outcrop and mineralogy of amphibole micaschist. Quartz (Qz), Biotite (Bt), Feldspar (Fsp), Plagioclase (Pl), Microcline (Mcc), Chlorite (Chl), Muscovite (Ms), and Garnet (Grt); minerals' abbreviations are according to [27].

- The garnet mica schist OD130 is located in the southern SSZ. It is affected by an axial-plane schistosity oriented NNE-SSW, overlain by a N-S schistosity certainly related to the shearing of the SSZ (**Figure 4(c)**). In thin section, the texture is granoblastic and the schistosity is well marked by all the minerals (quartz, feldspars, biotite, garnet, muscovite, tourmaline, and opaque minerals; **Figure 4(d)** and **Figure 4(e)**). The small subautomorphic quartz and feldspar crystals (approximately 70%) are surrounded by a mesostasis consisting

mainly of biotite and rare fibrous muscovite crystals (approximately 25%) (**Figure 4(d)**) and **Figure 4(e)**).

- The amphibole-bearing mica-schist OD104 was observed at the boundary of the deformed units of the SSZ, corresponding to the beginning of the SSZ eastern subdomain's migmatites (**Figure 4(f)**). Under transmitted light microscopy, the rock exhibits approximately 65% of quartz crystals, and feldspars minerals (plagioclase and microcline), which are the most abundant, and a schistosity marked by a preferential orientation of biotite and hornblende (approximately 30%) (**Figure 4(g)**). The hornblende is sometimes transformed into actinolite or chlorite. Accessory minerals include epidote and opaques (**Figure 4(g)**).
- The mylonite quartzite TOU081 was observed in the Sassandra River bed. It appears as a greenish-black slab with fine grains, and affected by millimetric penetrative schistosity and disjointed fractures (**Figure 5**). Under transmitted light microscopy, it has a mylonitic texture with a mineralogical assemblage consisting of feldspars, quartz, biotite, sphene and opaque minerals (**Figure 5**). About 95% of the rock is composed of laminated plagioclase and quartz. These minerals exhibit two types according to grain size including porphyroclasts and recrystallized subgrains (**Figure 5**). Porphyroclasts are generally deformed and associated with quartz-feldspathic sub-grains (**Figure 5**).

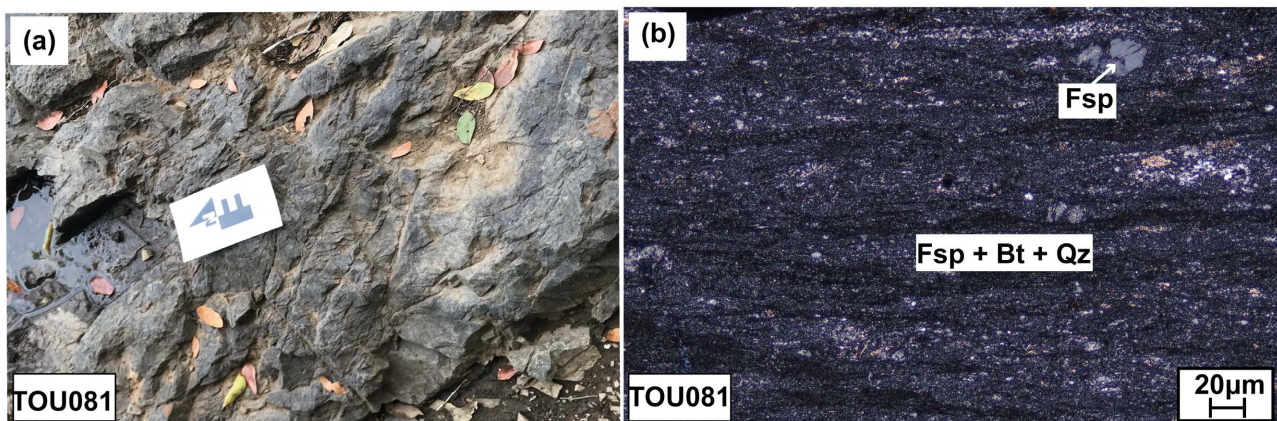


**Figure 5.** Photography and microphotography (under transmitted light) of the mylonite quartzite of the Sassandra River. Quartz (Qz), Biotite (Bt) and Feldspar (Fsp): minerals' abbreviations are according to [27].

## 4.2. Geochemical Data

### 4.2.1. Composition in Major and Trace Elements

The different concentrations of major and trace elements are recorded in **Table 1**. The SiO<sub>2</sub> compositions of the metasediments are between 50.5% and 75.08%, with Al<sub>2</sub>O<sub>3</sub> contents ranging between 12.24% and 17.16%. The alkali content (Na<sub>2</sub>O + K<sub>2</sub>O) is between 2.57% and 8.81%. The losses on ignition are quite low, around 1, except for the mylonite quartzite of the Sassandra River (TOU081), which is at 1.17%. The other major elements have the following proportions: Fe<sub>2</sub>O<sub>3</sub> (3.85% - 13.75%); MgO (0.61% - 5.05%); CaO (0.73% - 9.7%); Na<sub>2</sub>O (0.67% - 4.5%); MnO

(0.04% - 1.11%);  $K_2O$  (1.79% - 7.47%);  $TiO_2$  (0.38% - 1.31%) and  $P_2O_5$  (0.064% - 0.197%). The diagram in **Figure 6(a)** indicates that the rocks studied are of sedimentary origin with a well-marked peraluminous character [10]. Additionally, the diagrams in **Figure 6(b)** confirm this origin ([36] and [37]). According to the diagram in **Figure 6(c)**, the samples are mainly sandstones (wacke) and lith-arenites and incidentally shales [38].

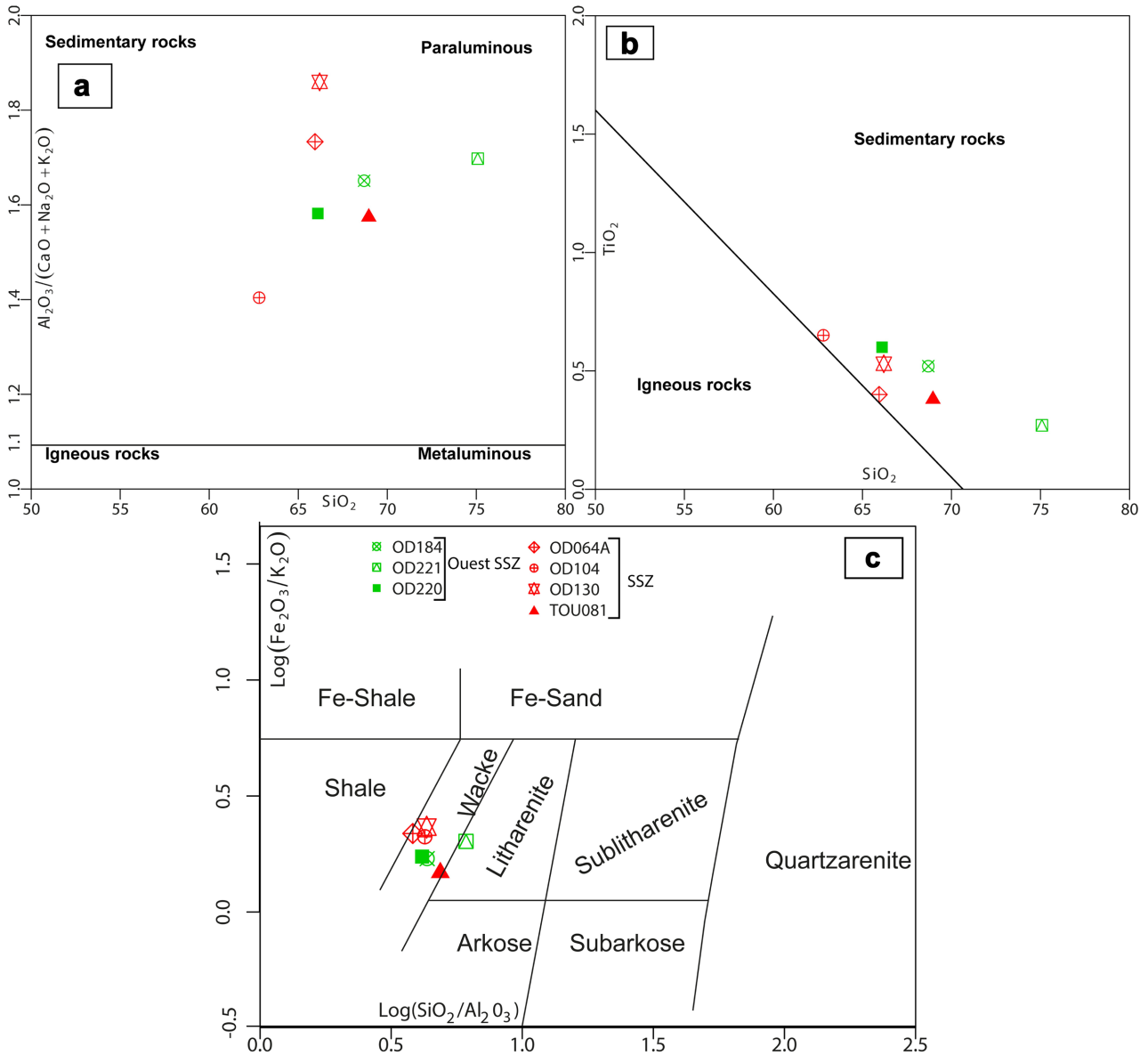


**Figure 6.** (a) Discrimination diagram of [10], (b)  $TiO_2$  versus  $SiO_2$  diagram of [37] and (c)  $\log(Na_2O/K_2O)$  versus  $\log(SiO_2/Al_2O_3)$  diagram of [38] applied to metasediments from northwestern part of Côte d'Ivoire.

The multi-element spectra of the western samples in green, and the SSZ in red, show slight and different variations (**Figure 7(a)**). The spectra of the incompatible lithophile elements or LILE (Ba, Rb, Th and U) show two isotopic trends: a positive anomaly (Ba and U), and a negative anomaly (Rb and Th) for the SSZ samples,

while there is a negative Ba anomaly for those from the west (**Figure 7(a)**). The multi-element spectra normalized to the primitive mantle in **Figure 7(a)**, present remarkable negative anomalies in Nb, Ta, P and Ti [39]. Additionally, the negative anomalies in Ti and P of the whole spectra, may be due to the fractionation of ilmenite and apatite. These geochemical signatures are characteristic of magmas generated in subduction zones or from the melting of a pre-existing continental crust. Furthermore, the SSZ samples, compared to those from the west, show a very homogeneous appearance of these spectra and could reflect the signature of the same source, having fed their sediments at the same time (**Figure 7(a)**).

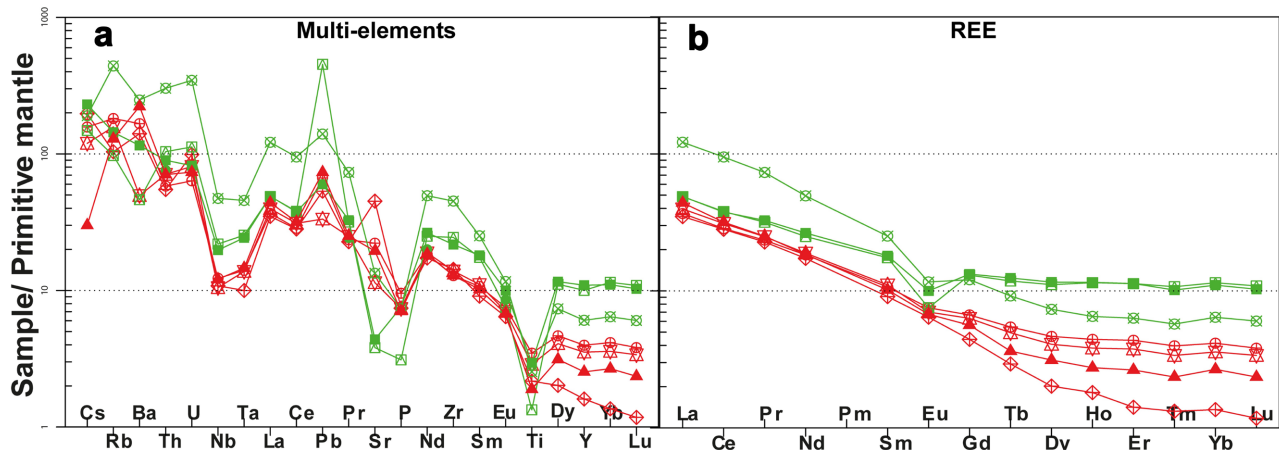


**Figure 7.** Multi-element (a) and rare earth (b) spectra applied to metasediments from the northwestern part of Côte d'Ivoire.

As for the rare earth or REE spectrum, all the samples evolve from lanthanum (La) to gadolinium (Gd) (**Figure 7(b)**). The spectra of the samples are characterized by a significant fractionation in LREE/HREE (**Figure 7(b)**). However, the rocks in the western part of the area, show a strongly negative anomaly in europium for its metasediments, while those located inside the SSZ, showing a very weak to almost zero anomaly in europium (**Figure 7(b)**). In addition, this negative anomaly in Eu, generally well-marked for the metasediments in the west and an enrichment in HREE unlike those of the SSZ, is typical of sediments of continental origin [40].

#### 4.2.2. Nature and Origin of Metasediments

The degree of alteration of the source rock can be assessed from the chemical index of alteration (CIA) based on the following molar proportions:  $CIA = [Al_2O_3 / (Al_2O_3 + CaO^\sigma + Na_2O + K_2O)] * 100$  ( $CaO^\sigma$ , corresponding to the concentration of CaO incorporated in the silicate fraction of the rock) [41]. Rocks with CIA values > 92 are highly altered due to the transformation of feldspars into clay minerals [42]. Rocks with CIA values between 60 and 80 show weathering, and those with CIA < 60 show, no or little weathering [43] [44]. The studied samples have CIA values ranging from 50.78 - 65.03, indicating low weathering of sediments, resulting from the disintegration of the source rocks (**Figure 8(a)**). The index (CIA) associated with the ternary A-CN-K diagram, provides information on the

intensity of the alteration as well as the composition of the original rock that gave rise to the sediments [44]. This index highlights a weak transformation of plagioclases into clays (Figure 8(a)). According to the ternary A-CN-K diagram coupled with the CIA index in Figure 8(a), the metasediments of the Odienné and Touba regions would come from rocks with compositions between gabbros (basalt) and granites, and presenting a weak to moderate alteration [41] [45]. The heterogeneous composition of the studied rocks is corroborated by the diagram ([36]), in which the samples show a distribution in the fields of sedimentary rocks (Figure 6(a) and Figure 6(b)).

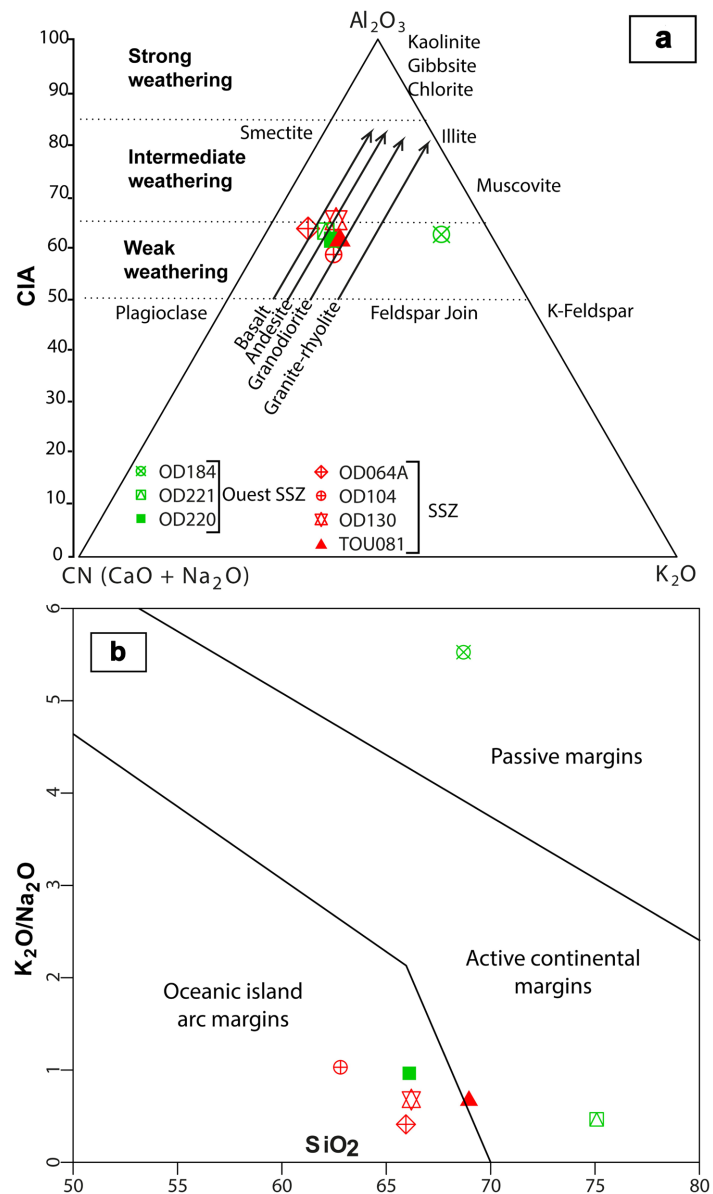


**Figure 8.** (a) A-CN-K diagram of [41] [45] as a function of  $CIA = [Al_2O_3 / (Al_2O_3 + CaO^* + Na_2O + K_2O)] \times 100$  of [17], the variables are expressed in molar proportion and (b)  $Na_2O/K_2O$  diagram as a function of  $SiO_2$  of [5] [46] applied to the metasediments of the northwestern part of Côte d'Ivoire.

### 4.2.3. Geotectonic Environment of Metasediments

Field data show an association of metasediments with metavolcanic rocks intruded by mafic, intermediate to felsic plutons. Most classifications related to metasediments highlight the existence of a correlation between the composition of detrital sediments and their geodynamic environments of deposition. Thus, the diagram in **Figure 8(b)** indicates that metasediments belong to three domains: the oceanic island arc margin domain, the active continental margin domain, and the passive margin domain [46].

## 5. Discussion

The petrographic study of the metasediments in the north-western part of Côte d'Ivoire (Odienné and Touba regions) shows a diversity of rocks, the main ones being micaschists, quartzite-mylonites, and paragneisses. Paragneiss minerals include quartz, feldspar, biotite, sillimanite, tourmaline, and a few opaque minerals such as ilmenite. Micaschists are made up of quartz, biotite, garnet, plagioclase, amphibole, rare chlorite, and a few tourmalines and ilmenites. Finally, quartzite-mylonite is rich in quartz and feldspar, with some biotite. The presence of certain metamorphic minerals, such as sillimanite, confirmed the sedimentary origin of the samples. Most of these metasediments have shales and sandstones as their protolith. This study also showed a geodynamic environment of the oceanic island arc margin and an active to passive continental margin type for its metasediments. Work carried out in the study area shows the presence of paragneiss and micaschist with identical mineralogical assemblage, except for the presence of staurotide [1]. In addition, work carried out in the SASCA area (south-west Côte d'Ivoire; Comoé basin) also shows the presence of garnet, staurotide, sillimanite and cordierite paragneisses ([47] [48]), and garnet and sillimanite paragneisses for the metasediments [49]. The estimated metamorphic conditions in our study area are amphibolite facies [1]. Some of these formations have also been observed in other birimian basins: Siguiri basin in Guinea ([50] [51]), Cape Coast in Ghana ([52]), and Bandama in Côte d'Ivoire ([53]). Furthermore, the majority of Birimian basins are composed of sandstone and claystone [42] [52]. The study area is thought to be made up of several small birimian basins [54] because the rocks studied are mainly composed of sandstones and lith-arenites. Furthermore, in our study area some others ([1]) indicate that the reworking or deformation of the pebbles could imply that the meta-conglomerates (OD253, **Figure 2**) represent the youngest terms of the sedimentary series to the northwest and that the Pb-Pb age on the zircons would be 2096 Ma obtained on a granitic pebble, representing the maximum limit of deposition [28]. Furthermore, new isotopic geochemistry data from Senegal show that Birimian rocks (Mako volcanic and Dialé-Daléma sedimentary) exhibit uniform juvenile characteristics with low initial Sr isotopic composition (0.700 to 0.704), positive Nd(t) values (2.1 to 4.3) and restricted Nd model ages (2.0 to 2.3 Ga) [55]. The triangular A-CN-K diagram of the rocks studied indicates that the protoliths evolve between basalts and granites (mixed vol-

canic and plutonic protoliths) after very little alteration (for sandstones) and little to moderate alteration (for shales) of the source rock indicated by the CIA alteration indices [44]-[56]. These results corroborate with certain works ([1]), which show an alteration and a recrystallization of the sediments of mafic to intermediate rocks for the biotite-amphibole-garnet micaschists in the western sector of Odienné. These results are similar to work on the Comoé basin, which reveals the existence of metasediments whose protoliths are thought to be intrusive (gabbros to granite) [49] [57]. In addition, in the southwestern basin of Côte d'Ivoire, more precisely in the SASCA domain, the same protoliths are present with a smaller interval (basalt to andesite) [47]. The geotectonic environment of an oceanic island arc and/or active continental margin highlighted by the geochemical study of the metasediments studied is corroborated by several studies, including those of [47]-[49] [57]. However, we have only one muscovite-rich metasediment seen on the western side of the SSZ (an area considered Archean to date), which falls within the field of passive margins. Only trace elements make it possible to distinguish the western domain from that of the SSZ in north-western of Côte d'Ivoire through Eu's anomaly (Figure 7). These metasediments were probably generated in the Paleoproterozoic (Birimian). While some studies indicate that there were no plate tectonics during this period ([58] [59]), various other studies stipulate that the Paleoproterozoic is more of a transition period in the evolution of crustal accretion processes [8] [60]. Of course, the quantity of samples analysed by isotope geochemistry will not allow us to discuss the geotectonics, but they will give us an objective idea of the geodynamic conditions that prevailed in the north-western sector of Côte d'Ivoire. The geotectonic environments highlighted by this work may therefore be debatable. Indeed, future work will allow us to confirm or refute this geodynamic context and/or better understand the tectonic style in the northwest of Côte d'Ivoire.

## 6. Conclusion

This study, focusing on the metasediments of the northwest of Côte d'Ivoire (Archean-Paleoproterozoic transition domain), specifically in the localities of Odienné and Touba, contributes to improving the geological knowledge of this sector, which remains poorly known to date. The metasediments studied are composed of micaschists, paragneisses, and mylonite quartzites. The micaschists are distinguished by the following mineral assemblage: quartz, feldspars, garnet, and biotite. The paragneisses are also made up of sillimanite. The different classifications of these metasediments based on the major elements reveal a belonging to the group of sandstones with a small component of shales and lith-arenites. The alteration index (CIA) is low to medium, ranging from 50 to 65, indicating low atmospheric alteration of the source rocks that produced these metasediments, the protoliths of which could be basalts, andesites, granodiorites, and granites. It should be noted that the samples from the SSZ have higher CIA alteration index values, while those from other areas are rather low to moderate. Although debat-

able, the geodynamic environments of these metasediments are of the oceanic island arc margin and active and passive continental margin type. Field data show the presence of metasediments in the vicinity of metavolcanic rocks, all intruded by granitoids. All these rocks form units, greenstone belts in this region (fertile formations), whose in-depth study could highlight the presence of interesting indicators in terms of mineralisation.

## Acknowledgements

This work is part of a doctoral study funded by the WAXI (West African eXploration Initiative) project in collaboration with the Agate project, the Geology and Mining Resources laboratory of the UFR STRM of the Félix Houphouët Boigny University of Cocody, Abidjan, Côte d'Ivoire and the LMI-MINERWA (Laboratoire Mixte International-Laboratory for Responsible Mining in West Africa) project.

## Conflicts of Interest

The authors declare no conflicts of interest regarding the publication of this paper.

## References

- [1] Caby, R., Delor, C. and Agoh, O. (2000) Lithologie, structure et métamorphisme des formations birimiennes dans la région d'Odienné (Côte d'Ivoire): Rôle majeur du diapirisme des plutons et des décrochements en bordure du craton de Man. *Journal of African Earth Sciences*, **30**, 351-374. [https://doi.org/10.1016/s0899-5362\(00\)00024-5](https://doi.org/10.1016/s0899-5362(00)00024-5)
- [2] Djro, S.C. (1998) Evolution tectono-métamorphiques des gneiss granulitiques archéens du secteur de Biankouma. Thèse de doctorat d'état, Ès Sciences Naturelles, Université Abidjan, 171 p.
- [3] Pothin, K.B. (1993) Un exemple de volcanisme du Protérozoïque inférieur en Côte d'Ivoire: Zone de subduction ou zone de cisaillement? *Journal of African Earth Sciences (and the Middle East)*, **16**, 437-443. [https://doi.org/10.1016/0899-5362\(93\)90102-v](https://doi.org/10.1016/0899-5362(93)90102-v)
- [4] Yacé, I. (1993) Les complexes volcano-sédimentaires précambriens en Afrique de l'Ouest. Publications Occasionnelles-Centre International pour la Formation. Échanges Géologiques, 94-96.
- [5] Roser, B.P. and Korsch, R.J. (1988) Provenance Signatures of Sandstone-Mudstone Suites Determined Using Discriminant Function Analysis of Major-Element Data. *Chemical Geology*, **67**, 119-139. [https://doi.org/10.1016/0009-2541\(88\)90010-1](https://doi.org/10.1016/0009-2541(88)90010-1)
- [6] Thiéblemont, D. (2001) A 3.5 Ga Granite-Gneiss Basement in Guinea: Further Evidence for Early Archean Accretion within the West African Craton. *Precambrian Research*, **108**, 179-194. [https://doi.org/10.1016/s0301-9268\(00\)00160-1](https://doi.org/10.1016/s0301-9268(00)00160-1)
- [7] Bessoles, B. (1977) Géologie de l'Afrique. Le craton ouest africain. Mém. B.R.G.M., n°88 Orléans (France). 402 p.
- [8] Kouamelan, A.-N. (1996) Géochronologie et Géochimie des Formations Archéennes et Protérozoïques de la Dorsale de Man en Côte d'Ivoire. Implications pour la Transition Archéen-Protérozoïque. Ph.D. Thesis, Université Rennes 1.
- [9] Tagini, B. (1971) Esquisse structurale de la Côte d'Ivoire. Essai de géotectonique régionale. Thèse de doctorat, Fac. Sci. Université Lausanne, Rapp. SODEMI, Abidjan, 266 p.

- [10] White, A.J.R. and Chappell, B.W. (1977) Ultrametamorphism and Granitoid Genesis. *Tectonophysics*, **43**, 7-22. [https://doi.org/10.1016/0040-1951\(77\)90003-8](https://doi.org/10.1016/0040-1951(77)90003-8)
- [11] Caen-Vachette, M., Tempier, P. and Camil, J. (1984) Age Rb/Sr de 1670 M.a. pour les mylonites de l'accident du Sassandra (Côte d'Ivoire) conséquence pour la datation des mouvements fini-éburnéens dans le craton ouest-africain. *Journal of African Earth Sciences* (1983), **2**, 359-363. [https://doi.org/10.1016/0899-5362\(84\)90009-5](https://doi.org/10.1016/0899-5362(84)90009-5)
- [12] Camil, J. (1984) Pétrographie, chronologie des ensembles granulitiques archéens et formations associées de la région de Man Côte d'Ivoire. Implication pour l'histoire géologique du craton Ouest-africain. These D'Etat University Abidj.
- [13] Camil, J. (1981) Un exemple de métamorphisme prograde de la base du faciès des amphibolites au faciès des granulites dans la région de man (Ouest de la Côte-d'Ivoire). Un ex. Metamorph. Prograde base faciès amphibolites au faciès granulites dans reg. Man ouest Côte-d'Ivoire. *Comptes Rendus de l'Académie Sciences Paris*, **293**, 513-518.
- [14] Koffi, G.R., Kouamelan, A.N., Allialy, M.E., Coulibaly, Y. and Peucat, J. (2020) Re-evaluation of Leonian and Liberian Events in the Geodynamical Evolution of the Man-Leo Shield (west African Craton). *Precambrian Research*, **338**, Article 105582. <https://doi.org/10.1016/j.precamres.2019.105582>
- [15] Kouamelan, A.N., Djro, S.C., Allialy, M.E., Paquette, J. and Peucat, J. (2015) The Oldest Rock of Ivory Coast. *Journal of African Earth Sciences*, **103**, 65-70. <https://doi.org/10.1016/j.jafrearsci.2014.12.004>
- [16] Vidal, M., Gumiaux, C., Cagnard, F., Pouclet, A., Ouattara, G. and Pichon, M. (2009) Evolution of a Paleoproterozoic "Weak Type" Orogeny in the West African Craton (ivory Coast). *Tectonophysics*, **477**, 145-159. <https://doi.org/10.1016/j.tecto.2009.02.010>
- [17] Doumbia, S., Pouclet, A., Kouamelan, A., Peucat, J.J., Vidal, M. and Delor, C. (1998) Petrogenesis of Juvenile-Type Birimian (Paleoproterozoic) Granitoids in Central Côte-D'ivoire, West Africa: Geochemistry and Geochronology. *Precambrian Research*, **87**, 33-63. [https://doi.org/10.1016/s0301-9268\(97\)00201-5](https://doi.org/10.1016/s0301-9268(97)00201-5)
- [18] Egal, E., Thiéblemont, D., Lahondère, D., Guerrot, C., Costea, C.A., Iliescu, D., et al. (2002) Late Eburnean Granitization and Tectonics along the Western and Northwestern Margin of the Archean Kénéma-Man Domain (Guinea, West African Craton). *Precambrian Research*, **117**, 57-84. [https://doi.org/10.1016/s0301-9268\(02\)00060-8](https://doi.org/10.1016/s0301-9268(02)00060-8)
- [19] Kouamelan, A.N., Delor, C. and Peucat, J. (1997) Geochronological Evidence for Re-working of Archean Terrains during the Early Proterozoic (2.1 Ga) in the Western Côte d'ivoire (Man Rise-West African Craton). *Precambrian Research*, **86**, 177-199. [https://doi.org/10.1016/s0301-9268\(97\)00043-0](https://doi.org/10.1016/s0301-9268(97)00043-0)
- [20] Gasquet, D., Barbey, P., Adou, M. and Paquette, J.L. (2003) Structure, Sr-Nd Isotope Geochemistry and Zircon U-Pb Geochronology of the Granitoids of the Dabakala Area (Côte d'ivoire): Evidence for a 2.3 Ga Crustal Growth Event in the Palaeoproterozoic of West Africa? *Precambrian Research*, **127**, 329-354. [https://doi.org/10.1016/s0301-9268\(03\)00209-2](https://doi.org/10.1016/s0301-9268(03)00209-2)
- [21] Gouedji, F., Picard, C., Coulibaly, Y., Audet, M., Auge, T., Goncalves, P., et al. (2014) The Samapleu Mafic-Ultramafic Intrusion and Its Ni-Cu-PGE Mineralization: An Eburnean (2.09 Ga) Feeder Dyke to the Yacouba Layered Complex (Man Archean Craton, Western Ivory Coast). *Bulletin de la Société Géologique de France*, **185**, 393-411. <https://doi.org/10.2113/gssgfbull.185.6.393>
- [22] Koffi, A.Y., Baratoux, L., Pitra, P., Kouamelan, A.N., Vanderhaeghe, O., Thébaud, N., et al. (2023) A Tectonic Model for the Juxtaposition of Granulite- and Amphibolite-

- Facies Rocks in the Eburnean Orogenic Belt (Sassandra-Cavally Domain, Côte d'Ivoire). *BSGF-Earth Sciences Bulletin*, **194**, Article 11.  
<https://doi.org/10.1051/bsgf/2023007>
- [23] Kouamelan, A.N., Kra, K.S.A., Djro, S.C., Paquette, J. and Peucat, J. (2018) The Logoualé Band: A Large Archean Crustal Block in the Kenema-Man Domain (man-Leo Rise, West African Craton) Remobilized during Eburnean Orogeny (2.05 Ga). *Journal of African Earth Sciences*, **148**, 6-13.  
<https://doi.org/10.1016/j.jafrearsci.2017.09.004>
- [24] Liégeois, J.P., Claessens, W., Camara, D. and Klerkx, J. (1991) Short-Lived Eburnian Orogeny in Southern Mali. *Geology, Tectonics, U-Pb and Rb-Sr Geochronology. Precambrian Research*, **50**, 111-136. [https://doi.org/10.1016/0301-9268\(91\)90050-k](https://doi.org/10.1016/0301-9268(91)90050-k)
- [25] Pitra, P., Kouamelan, A.N., Ballèvre, M. and Peucat, J. (2010) Palaeoproterozoic High-Pressure Granulite Overprint of the Archean Continental Crust: Evidence for Homogeneous Crustal Thickening (Man Rise, Ivory Coast). *Journal of Metamorphic Geology*, **28**, 41-58. <https://doi.org/10.1111/j.1525-1314.2009.00852.x>
- [26] Bonhomme, M. (1962) Contribution à l'étude géochronologique de la plate-forme de l'Ouest Africain. Imprimerie Louis-Jean.
- [27] Warr, L.N. (2021) IMA-CNMNC Approved Mineral Symbols. *Mineralogical Magazine*, **85**, 291-320. <https://doi.org/10.1180/mgm.2021.43>
- [28] Feybesse, J.-L., Milési, J.-P., Johan, V., Dommanget, A., Calvez, J.-Y., Boher, M. and Abouchami, W. (1989) La limite Archéen/Protérozoïque inférieur d'Afrique de l'Ouest: Une zone de chevauchement majeure antérieure à l'accident de Sassandra; l'exemple des régions d'Odiénné et de Touba (Côte-d'Ivoire). *Lt. ArchéenProtéro-zoïque Infér. Afr. Ouest Une Zone Chevauchement Majeure Antérieure À Accid. Sassandra Ex. Régions Odiénné Touba Côte-d'Ivoire*, **309**, 1847-1853.
- [29] Lemoine, S. (1988) Evolution de la région de Dabakala (NE de la Côte d'Ivoire) au Protérozoïque inférieur. Possibilités d'extension au reste de la Côte d'Ivoire et au Burkina Faso. Similitudes et différences; les linéaments de Green-ville-Ferkessedougou et grand CessNiakaramandougou. PhD Thesis, Thèse de Doctorat ès Sciences Naturelles, Université Clermont Ferrand II, France.
- [30] Abouchami, W., Boher, M., Michard, A. and Albarede, F. (1990) A Major 2.1 Ga Event of Mafic Magmatism in West Africa: An Early Stage of Crustal Accretion. *Journal of Geophysical Research: Solid Earth*, **95**, 17605-17629.  
<https://doi.org/10.1029/jb095ib11p17605>
- [31] Boher, M., Abouchami, W., Michard, A., Albarede, F. and Arndt, N.T. (1992) Crustal Growth in West Africa at 2.1 Ga. *Journal of Geophysical Research: Solid Earth*, **97**, 345-369. <https://doi.org/10.1029/91jb01640>
- [32] Pouclet, A., Vidal, M., Doumnang, J.-C., Vicat, J.-P. and Tchameni, R. (2006) Neoproterozoic Crustal Evolution in Southern Chad: Pan-African Ocean Basin Closing, Arc Accretion and Late- to Post-Orogenic Granitic Intrusion. *Journal of African Earth Sciences*, **44**, 543-560. <https://doi.org/10.1016/j.jafrearsci.2005.11.019>
- [33] Koffi, A.Y., Thébaud, N., Kouamelan, A.N., Baratoux, L., Bruguier, O., Vanderhaeghe, O., *et al.* (2022) Archean to Paleoproterozoic Crustal Evolution in the Sassandra-Cavally Domain (Côte d'Ivoire, West Africa): Insights from Hf and U-Pb Zircon Analyses. *Precambrian Research*, **382**, Article 106875.  
<https://doi.org/10.1016/j.precamres.2022.106875>
- [34] Milési, J.P., Feybesse, J.L., Pinna, P., Deschamps, Y., Kampunzu, H., Muhongo, S., Lescuyer, J.L., Le Goff, E., Delor, C. and Billa, M. (2004) Geological Map of Africa 1: 10,000,000, SIGAfrique Project, in: 20th Conference of African Geology, BRGM, Or-

- léans, France. 2-7.
- [35] Thiéblemont, D., Liégeois, J.P., Fernandez-Alonso, M., Ouabadi, A., Le Gall, B., Maury, R., Jalludin, M., Vidal, M., Ouattara Gbélé, C. and Tchaméni, R. (2016) Geological Map of Africa at 1: 10M Scale. Geol. Map CGMW-BRGM.
- [36] Tarney, J., Saunders, A.D. and Weaver, S.D. (1977) Geochemistry of Volcanic Rocks from the Island Arcs and Marginal Basins of the Scotia Arc Region. In: *Maurice Ewing Series*, American Geophysical Union, 367-377.
- [37] Tarney, J. and Windley, B.F. (1977) Chemistry, Thermal Gradients and Evolution of the Lower Continental Crust. *Journal of the Geological Society*, **134**, 153-172. <https://doi.org/10.1144/gsjgs.134.2.0153>
- [38] Herron, M.M. (1988) Geochemical Classification of Terrigenous Sands and Shales from Core or Log Data. *SEPM Journal of Sedimentary Research*, **58**, 820-829. <https://doi.org/10.1306/212f8e77-2b24-11d7-8648000102c1865d>
- [39] McDonough, W.F. and Sun, S.-S. (1995) The Composition of the Earth. *Chemical Geology*, **120**, 223-253. [https://doi.org/10.1016/0009-2541\(94\)00140-4](https://doi.org/10.1016/0009-2541(94)00140-4)
- [40] Fezaa, N., Liégeois, J.P., Abdallah, N., Bruguier, O., Laouar, R. and Ouabadi, A. (2016) Origine du groupe métasédimentaire de Djanet (Hoggar oriental, Algérie). Géochronologie et géochimie. *Bulletin du Service Géologique de l'Algérie*, **24**, 3-26.
- [41] Nesbitt, H.W. and Young, G.M. (1984) Prediction of Some Weathering Trends of Plutonic and Volcanic Rocks Based on Thermodynamic and Kinetic Considerations. *Geochimica et Cosmochimica Acta*, **48**, 1523-1534. [https://doi.org/10.1016/0016-7037\(84\)90408-3](https://doi.org/10.1016/0016-7037(84)90408-3)
- [42] Potter, P.E., Maynard, J.B. and Depetris, P.J. (2005) Mud and Mudstones: Introduction and Overview. Springer Science & Business Media. <https://doi.org/10.1007/b138571>
- [43] Aristizábal, E., Roser, B. and Yokota, S. (2009) Patrones e índices de meteorización química de los depósitos de vertiente y rocas fuentes en el Valle de Aburrá. *Boletín de Ciencias de la Tierra*, **25**, 27-42.
- [44] Fedo, C.M., Wayne Nesbitt, H. and Young, G.M. (1995) Unraveling the Effects of Potassium Metasomatism in Sedimentary Rocks and Paleosols, with Implications for Paleoweathering Conditions and Provenance. *Geology*, **23**, 921-924. [https://doi.org/10.1130/0091-7613\(1995\)023<0921:uteopm>2.3.co;2](https://doi.org/10.1130/0091-7613(1995)023<0921:uteopm>2.3.co;2)
- [45] Nesbitt, H.W. and Young, G.M. (1989) Formation and Diagenesis of Weathering Profiles. *The Journal of Geology*, **97**, 129-147. <https://doi.org/10.1086/629290>
- [46] Roser, B.P. and Korsch, R.J. (1986) Determination of Tectonic Setting of Sandstone-Mudstone Suites Using SiO<sub>2</sub> Content and K<sub>2</sub>O/Na<sub>2</sub>O Ratio. *The Journal of Geology*, **94**, 635-650. <https://doi.org/10.1086/629071>
- [47] Koffi, A.M.P., Yacouba, C., Zié, O. and Inza, C. (2018) Caractéristiques pétrographiques et géochimiques des métasédiments de la partie sud-est du bassin de la comoé (nord d'alépé-sud est de la Côte d'ivoire). *Revue RAMReS*, **6**, 28-35.
- [48] Kouadio, B., Djeneb, C., Yvette, F.N.B., Yao, K., Basile, Y.A., Cynthia, Y.Y., Alain, A.S. and Noël, Z.G. (2016) Étude ethnobotanique des plantes médicinales utilisées dans le Département de Transua, District du Zanzan (Côte d'Ivoire). *Journal of Animal and Plant Sciences*, **27**, 4230-4250.
- [49] Adingra, M.P., Coulibaly, Y., Ouattara, Z. and Coulibaly, I. (2018) Caractéristiques pétrographiques et géochimiques des métasédiments de la partie sud-est du bassin de la comoé (nord d'alépé-sud est de la Côte d'ivoire). *Science de la vie, de la terre et agronomie*, **6**.

- [50] Feybesse, J.L., Billa, M., Diaby, S., Diallo, S., Egal, E., Le Metour, J., Lescuyer, J.L., Sylla, B.I. and Villeneuve, M. (2004) Notice explicative de la Carte Géologique et Géologique à 1/500,000 de la Guinée. BRGM, DNRGH, 60.
- [51] Feybesse, J., Billa, M., Guerrot, C., Duguey, E., Lescuyer, J., Milesi, J., *et al.* (2006) The Paleoproterozoic Ghanaian Province: Geodynamic Model and Ore Controls, Including Regional Stress Modeling. *Precambrian Research*, **149**, 149-196. <https://doi.org/10.1016/j.precamres.2006.06.003>
- [52] Asiedu, D.K., Asong, S., Atta-Peters, D., Sakyi, P.A., Su, B., Dampare, S.B., *et al.* (2017) Geochemical and Nd-Isotopic Compositions of Juvenile-Type Paleoproterozoic Birimian Sedimentary Rocks from Southeastern West African Craton (Ghana): Constraints on Provenance and Tectonic Setting. *Precambrian Research*, **300**, 40-52. <https://doi.org/10.1016/j.precamres.2017.07.035>
- [53] Doumbia, S. (1997) Géochimie, géochronologie et géologie structurale des formations birimiennes de la région de Katiola-marabadiassa (centre nord de la Côte d'Ivoire): Evolution magmatique et contexte géodynamique du paleoproterozoïque. Ph.D., Natural Sciences, Abidjan University, Éd. BR.M. n°276, 207 p.
- [54] Asiedu, D.K., Dampare, S.B., Sakyi, P.A., Banoeng-Yakubo, B., Osae, S., Nyarko, B.J.B., *et al.* (2004) Geochemistry of Paleoproterozoic Metasedimentary Rocks from the Birim Diamondiferous Field, Southern Ghana: Implications for Provenance and Crustal Evolution at the Archean-Proterozoic Boundary. *GEOCHEMICAL JOURNAL*, **38**, 215-228. <https://doi.org/10.2343/geochemj.38.215>
- [55] Pawlig, S., Gueye, M., Klischies, R., Schwarz, S., Wemmer, K. and Siegesmund, S. (2006) Geochemical and Sr-Nd Isotopic Data on the Birimian of the Kedougou-Kenieba Inlier (Eastern Senegal): Implications on the Palaeoproterozoic Evolution of the West African Craton. *South African Journal of Geology*, **109**, 411-427. <https://doi.org/10.2113/gssaig.109.3.411>
- [56] Roddaz, M., Debat, P. and Nikiema, S. (2007) Geochemistry of Upper Birimian Sediments (Major and Trace Elements and Nd-Sr Isotopes) and Implications for Weathering and Tectonic Setting of the Late Paleoproterozoic Crust. *Precambrian Research*, **159**, 197-211. <https://doi.org/10.1016/j.precamres.2007.06.008>
- [57] Boya, T.K.L.-D., Kouadio, F.J.L.H., Adingra, M.P.K., N'gatta, K.G.-L. and Kouame-lan, A.N. (2022) Les métasédiments de Kouassi Bilékro, S/P de Kouassi Datékro, Est de la Côte d'Ivoire: Un exemple de pétrogénèse complexe au sein du bassin de la Comoé. *Africa Science*, **20**, 57-71.
- [58] Kusky, T.M. and Li, J. (2003) Paleoproterozoic Tectonic Evolution of the North China Craton. *Journal of Asian Earth Sciences*, **22**, 383-397. [https://doi.org/10.1016/s1367-9120\(03\)00071-3](https://doi.org/10.1016/s1367-9120(03)00071-3)
- [59] Trap, P. (2007) Style tectonique et contexte géodynamique au Paléoproterozoïque. Exemple du Craton de Chine du Nord. Ph.D. Thesis, Université d'Orléans.
- [60] Laurent, O. (2013) Les changements géodynamiques à la transition Archéen-Proterozoïque: Étude des granitoïdes de la marge Nord du craton du Kaapvaal (Afrique du Sud). Ph.D. Thesis, Université Blaise Pascal-Clermont-Ferrand II.